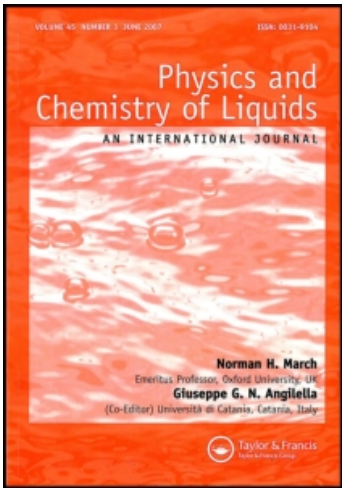

Physics and Chemistry of Liquids
Publication details, including instructions for authors and subscription information:
http://www.informaworld.com/smpp/title~content=t713646857

A Comparative Analysis of the Rice-Allnatt and Square-Well Liquid Transport Theories

I. B. Schrodt[a]; J. S. Ku[a]; K. D. Luks[a]
[a] Department of Chemical Engineering, University of Notre Dame Notre Dame, Ind.,

To cite this Article Schrodt, I. B. , Ku, J. S. and Luks, K. D.(1971) 'A Comparative Analysis of the Rice-Allnatt and Square-Well Liquid Transport Theories', Physics and Chemistry of Liquids, 2: 3, 147 — 163
To link to this Article: DOI: 10.1080/00319107108083809
URL: http://dx.doi.org/10.1080/00319107108083809

Physics and Chemistry of Liquids. 1971. Vol. 2, pp. 147–163

Printed in Great Britain

A Comparative Analysis of the Rice-Allnatt and Square-Well Liquid Transport Theories

I. B. SCHRODT, J. S. KU and K. D. LUKS

Department of Chemical Engineering
University of Notre Dame
Notre Dame, Ind. 46556

Abstract—The Yvon-Born-Green pair correlation function theory is discussed from the viewpoint of its role as theoretical data input for the Rice-Allnatt liquid transport theory. The general behavior of the Rice-Allnatt theory is shown to compare favorably with that of the square-well transport theory of Davis, Rice, and Sengers, although the former is not as quantitative. The predictive ability of the Rice-Allnatt theory is improved by a systematic adjustment of the Lennard-Jones parameters used in the YBG pair correlation functions, based on the critical point locus.

1. Introduction

With the advent of the computer, much attention has been paid to the prediction of equilibrium and non-equilibrium properties of fluids by the molecular approach. The bulk of this work has been directed to the imperfect and dense gas regimes (fluids at temperatures above the critical point; see Fig. 1) with only crude models and correlations being applied to liquids (fluids at temperatures below the critical point and densities above the critical density) with any degree of completeness and success.

To predict the equilibrium properties of a liquid by the molecular approach, one assigns to a fluid an intermolecular potential, whose parameters are usually determined from gaseous virial or transport data. This potential function is used to generate the pair correlation function, defined as:

$$g^{(2)}(\underline{r}_1, \underline{r}_2) = \frac{V^2(N-1)}{NZ} \int_V \cdots \int \exp(-U/kT)\, \mathrm{d}\underline{r}_3 \cdots \mathrm{d}\underline{r}_n \qquad (1)$$

where U is the total intermolecular potential of the N-body systems and Z is the configurational partition function. This correlation

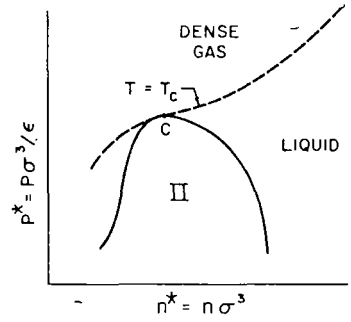

Figure 1 A schematic diagram of the dense gas and liquid regimes, where P^* is the reduced pressure, n^* is the reduced density, T^* is the reduced temperature and II denotes the two phase region. c refers to the critical point.

function can be used to predict all the thermodynamic properties of the liquid, e.g., the pressure is expressed as:

$$P = \frac{NkT}{V}\left\{1 - \frac{2N\pi}{3VkT}\int_0^\infty r^3 u'(r)\, g^{(2)}(r)\, \mathrm{d}r\right\} \tag{2}$$

where $u'(r)$ is the derivative of the intermolecular potential. There are many integral equations that have been used to generate $g^{(2)}(r)$ in the dense gas regime; those few that have been tested in the liquid regime will be discussed in section 2. Using only the experimental information contained in the intermolecular potential to predict properties is referred to as " a priori prediction ". The prediction of liquid transport properties requires a description of the collision mechanism, usually a kinetic equation analogous to the dilute gas Boltzmann equation. Examples of liquid kinetic theories that have been developed are the square-well and Rice-Allnatt theories. The use of these theories, particularly the latter, requires knowledge of the equilibrium pair correlation function. Consequently, it seems logical that if one is to be successful in the prediction of liquid transport properties, one should have at least a qualitatively good liquid pair correlation function. It should be noted that the pressure and the transport coefficients have a very sensitive dependence on $g^{(2)}(r)$.

In section 2, the pair correlation function determination of the liquid regime is examined using the criterion of equal chemical potential of phases. Specifically, the locus of the phase transition en-

velope is examined. Section 3 extends the results of 2 to the liquid transport problem and qualitatively discusses the extent of agreement of the square-well and Rice-Allnatt theories with experiment. The scope of this paper is limited to " simple " liquids, i.e., classical non-polar spherical molecules, such as argon, krypton, xenon or methane.

2. The Pair Correlation Function; its Definition of the Liquid Regime

In order to predict successfully the equilibrium or transport properties of a liquid at or near saturation, a pair correlation function theory is needed which at least qualitatively describes the boundary between the liquid and the 2-phase region. See Fig. 2. The boundary between the stable liquid regime and the metastable 2-phase region is determined by the criterion

$$\mu_{\text{gas}} = \mu_{\text{liquid}} \text{ at some } P, T \tag{3}$$

which yields a saturated gas and a saturated liquid point on the phase envelope at the same pressure and temperature. Any equation of state can be inserted into the criterion, e.g., Eq. 2. The general use of this criterion is presented in detail by Callen.[1]

Kirkwood *et al.*[2] solved the Yvon-Born-Green (YBG) integral equation[3] for $g^{(2)}(\underline{r}_1, \underline{r}_2)$ using the modified Lennard-Jones potential

$$\begin{aligned} u(r) &= +\infty, \quad r < \sigma \\ &= 4\epsilon[(\sigma/r)^{12} - (\sigma/r)^{6}], \quad r \geqslant \sigma \end{aligned} \tag{4}$$

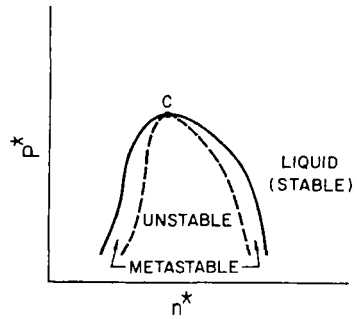

Figure 2. A schematic diagram showing the occurrence of the metastable, unstable and stable regimes for a pure substance.

and tabulated $g^{(2)}(\underline{r}_1, \underline{r}_2)$ as a function of temperature at several densities. Using the reduced temperature $T^* = Tk/\epsilon$ and density $n^* = n\sigma^3$, the YBG liquid phase envelope can be identified as a unique curve. See Fig. 3. By comparing this section of the saturated

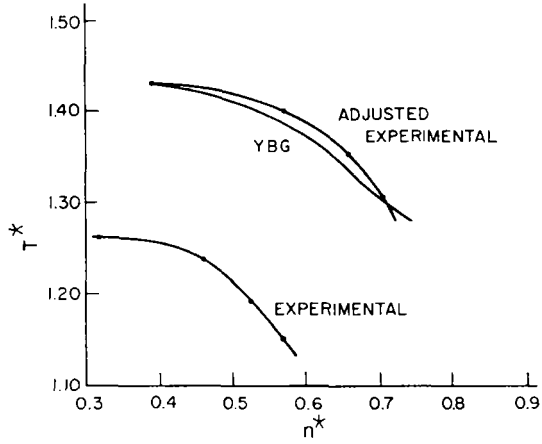

Figure 3. A comparison of the T^*–n^* curve for the saturated liquid state for argon (" Experimental "), based on molecular parameters obtained from second virial coefficient data, with that predicted by the YBG theory and also the adjusted experimental argon data.

liquid curve with the experimental curve for saturated liquid argon (using $\sigma = 3.405 \times 10^{-8}$ cm and $\epsilon = 1.653 \times 10^{-14}$ erg determined from second-virial-coefficient data to reduce the saturated liquid data), one sees that the experimental curve falls well within the two-phase region mapped out by the YBG theory. The consequence is that if one were to take an experimental density and temperature for saturated liquid argon, one would get a pressure from the YBG theory and Eq. 2 characteristic of the YBG metastable or unstable region.

Rice *et al.*[4] found negative pressures were obtained when they inserted saturated liquid argon data into the equation of state.† This results from the fact that the state isotherms of the YBG theory

† They used a slightly different set of parameters:

$$\sigma = 3.418 \times 10^{-8}\,\text{cm} \text{ and } \epsilon = 1.71 \times 10^{-14}\,\text{erg}.$$

often drop below the $P^* = 0$ axis in the two phase region.† Recognizing that the potential parameters determined from the gas data were unsatisfactory, they "scaled" the σ-parameter until $P_{YBG} = P_{experiment}$ and found a significant improvement in the prediction of transport properties for liquid argon by the Rice-Allnatt theory[4,5,6] (see Appendix B). The effect of this "scaling" was to move the experimental curve in Fig. 3 horizontally to the vicinity of the YBG theoretical curve.

The experimental argon curve in Fig. 3 not only is displaced from the YBG envelope along the density n^* axis but also there is substantial displacement with respect to T^*. For example, for the critical point, for the YBG theory.

$$n_c^* = 0.387$$

$$T_c^* = 1.433$$

as compared to the experimental locus $T_c^* = 1.261$, $n_c^* = 0.316$. Perhaps a more realistic method of scaling would be to adjust the experimental (n^*, T^*) phase envelope by matching the experimental (n_c^*, T_c^*) point to that of the YBG theory. The new potential parameters that will do this are

$$\sigma = 3.65 \times 10^{-8} \text{ cm}$$

$$\epsilon = 1.46 \times 10^{-14} \text{ erg}$$

The effect of changing parameters in this manner is to shift the experimental phase envelope to the vicinity of the YBG phase envelope. Figure 3 shows that the theory and the adjusted experimental data fall closely together. Use of the adjusted reduced variables (n^*, T^*) with the YBG theory will lead to predicted pressures characteristic of the liquid region close to the saturated liquid curve in the domain $1.30 < T^* < 1.40$. Of course, in contrast to Rice's scaling procedure, the theoretical and experimental pressures will not exactly match. See Fig. 4. The justification for using our technique is that it is felt that equilibrium data close to the saturated

† It should be noted that the above molecular parameters were obtained for the Lennard–Jones 12–6 potential and used in a version of the YBG theory devised for the modified Lennard–Jones 12–6 potential. Thus it cannot be stated with complete certainty that the pressures are negative for theoretical reasons alone.

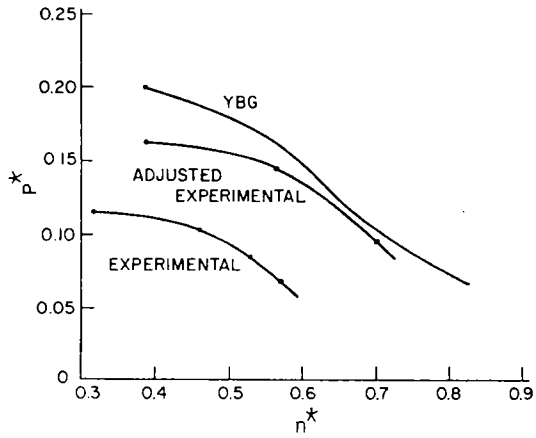

Figure 4. A comparison of the P^*-n^* curve for the saturated liquid state for argon (" Experimental "), based on molecular parameters obtained from second virial coefficient data, with that predicted by the YBG theory and also the adjusted experimental argon data.

liquid curve are needed to predict transport properties in the same state vicinity with any consistency. Because of the sharp drop (to negative values) in P_{YBG} in the 2-phase region, it is considered an advantage that the theory will predict pressures close to the one-phase region of the adjusted experimental (n^*, T^*) locus of the saturated liquid. Table I shows that the prediction of argon vapor pressure is very good at 140.4 °K and, although the YBG pressure at 122.7 °K is still negative, it is an improved prediction. This improvement will be more apparent in the prediction of transport properties in section 3.

In closing this discussion of equilibrium behavior it should be mentioned that use of the Percus-Yevick (PY) theory to define the liquid envelope was considered, because of the success of the PY theory in predicting the lower hard sphere virial coefficients in the dense gas regime. Rovner's work[7] with the PY theory using a standard Lennard-Jones 12-6 potential was corroborated, the essence of which is that the PY theory yields non-physical pressure predictions in the region of the saturated liquid curve. Further non-physical behavior was found when the intermolecular potential used in the Percus-Yevick theory was the modified Lennard-Jones potential in Eq. (4).[8] Our conclusion at present is that the YBG

TABLE 1 A comparison of the YBG theory and experiment for argon vapor pressure at two different densities with the second virial coefficient parameters ($\sigma = 3.405 \times 10^{-8}$ cm, $\epsilon = 1.653 \times 10^{-14}$ erg) and the adjusted parameters ($\sigma = 3.65 \times 10^{-8}$ cm, $\epsilon = 1.46 \times 10^{-14}$ erg).

Before Adjustment			
$\rho_m(g/cm^3)$	T (°K)	$P_{YBG(atm)}$	$P_{exp(atm)}$
1.16	120.3	−247.5	12.3
1.42	86.2	−961	0.9
After Adjustment			
$\rho_m(g/cm^3)$	T	P_{YBG}	P_{exp}
0.924	140.4	34.7	32.0
1.12	122.7	−175	13.8

theory is the only well-tested pair correlation function theory existing that qualitatively describes the liquid pressure behavior correctly at and near the phase transition envelope. It is felt that advantage can be taken of this qualitative agreement by an adjustment of the intermolecular potential parameters, leading to a subsequent improvement in the thermodynamic and transport property prediction.

3. A Comparison of Liquid Transport Theories

The development and solution of kinetic equations to obtain expressions for transport properties of dilute gases is well-known. The method has been extended to dense gases and liquids with some success.[9] As shown in section 2, pressure is a derived function of density and temperature. Likewise, transport coefficients such as shear viscosity and thermal conductivity are derived theoretically as functions of density and temperature, as opposed to the customary specifications of pressure and temperature of their actual measurement. Consequently, it is interesting to examine the density dependence of the transport properties of liquids assume. Diller *et al.*[10] have pointed out that the characteristic transport behavior of

classical liquids is represented by increases in thermal conductivity and decreases in shear viscosity with increasing temperature along constant density loci. (They preferred to use transport coefficient differences of the type $\Delta\eta = \eta - \eta^*$ where η is the liquid transport coefficient at temperature T and density n, and η^* is the dilute real gas transport coefficient of shear viscosity.) The behavior of liquid argon thermal conductivity is demonstrated in Fig. 5. The graphical behavior of shear viscosity is difficult to display clearly because of the closeness of the isotherms and the saturated liquid curve. From analysis of the shear viscosity data of de Bock *et al.*,[21] it appears that the stated criterion of $(\partial\eta/\partial T)_n^* < 0$ holds for liquids near saturation up to at least 120 °K. At 200 atm pressure or more, the behavior is not clear from the available data. The function $\Delta\eta$ has a stronger negative temperature derivative at constant density, but still it is difficult to display this behavior clearly in graphical form. For the sake of discussion, attention will be restricted to the total shear viscosity and thermal conductivity. A good transport theory

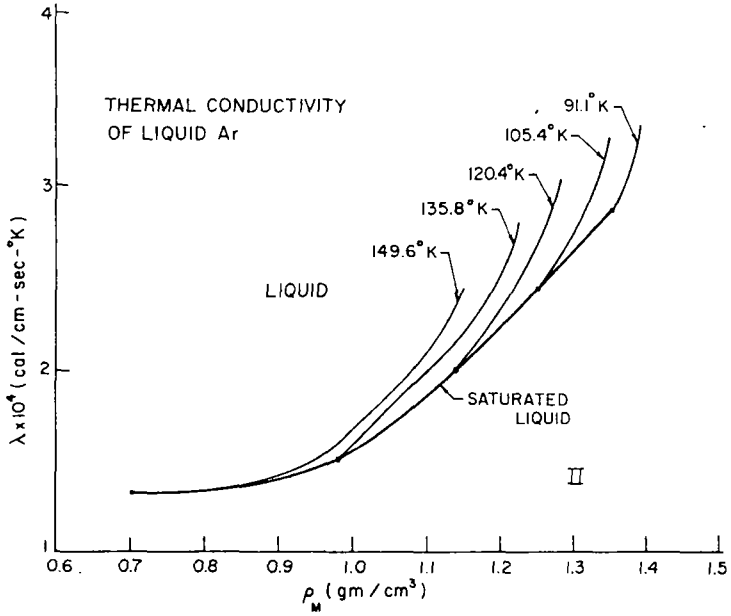

Figure 5. A diagram of the thermal conductivity of liquid argon as a function of mass density, devised from Ikenberry and Rice[19] and Cook.[20]

should at least qualitatively predict the experimental temperature dependence of the transport properties.

Two well-known liquid transport kinetic theories are the square-well theory of Davis, Rice and Sengers[11] and the Rice-Allnatt theory.[4,5,6] Both of these theories have been previously reviewed, but only the square-well theory has been extensively tested[12,13] against experiment. It is revealing to compare these two theories from the viewpoint of the behavior of their coefficients in the liquid regime in order to evaluate their " goodness " as transport descriptions for simple liquids.

The square-well theory is a modification of the Enskog theory for a dense gas of hard spheres; the mathematically simple square-well intermolecular potential is shown in Fig. 6. The square-well transport results are given in Appendix A.

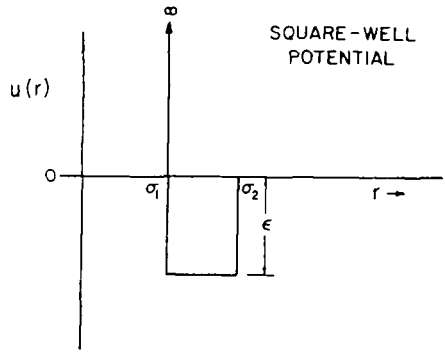

Figure 6. The square-well intermolecular potential model.

The traditional Enskog theory[14] predicts that shear viscosity and thermal conductivity behave as

$$\left(\frac{\partial \eta}{\partial T}\right)_{n^*} > 0 \tag{5}$$

and

$$\left(\frac{\partial \lambda}{\partial T}\right)_{n^*} > 0 \tag{6}$$

for all temperatures and density. The addition of the square-well to the hard sphere intermolecular potential causes the temperature coefficients in Eq. (5) and (6) to pass through a zero-value locus as

temperature is lowered. See Fig. 7. The effect is to give liquid shear viscosity the proper qualitative behavior, but in turn to cause liquid thermal conductivity to assume an unnatural trend upon lowering the temperature into the liquid regime (the turning point is at about 135 °K for liquid argon). Thus, the square-well theory should be satisfactory in a qualitative sense for liquid viscosity, but not for liquid thermal conductivity except at near critical temperatures. It is interesting to note that the square-well theory has demonstrated quantitative agreement for thermal conductivity for the inert liquids when compared with experiment.[12,13] This agreement is partly fortuitous. There is good agreement with experiment, e.g., for liquid Argon thermal conductivity at about 145 °K. The only reason why this agreement is still good at about 100 °K is precisely because the temperature coefficient of λ, Eq. 6, changes sign. The theoretical data once again achieves the proper magnitude of the experimental data, but this time, the wrong temperature coefficient.

The Rice-Allnatt theory, in contrast, displays proper behavior for both shear viscosity and thermal conductivity in the liquid regime.

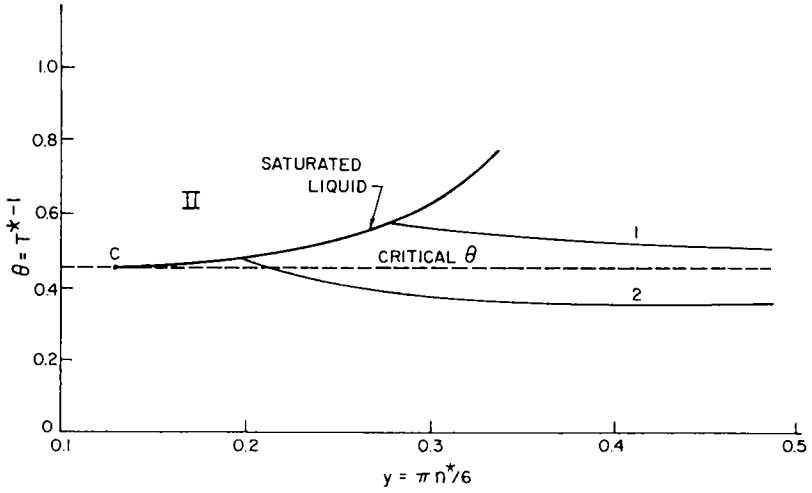

Figure 7. A θ–y diagram for the square-well model of transport denoting the liquid and dense gas regimes (separated by the critical θ line). Curve 1 denotes the line above which $(\partial\lambda/\partial T) < 0$ and below which $(\partial\lambda/\partial T) > 0$ for the square-well model. Curve 2 has a parallel interpretation for shear . cosity η c is the critical point.

See Figs. 8 and 9. The Rice-Allnatt theory, based on the collision mechanism of binary hard collisions followed by Brownian behavior of the molecules in a many body environment, is summarized in Appendix B. As the computations used for Figs. 9 and 10 are new and show some variation with previous work, the method of calculation of the Rice-Allnatt properties is briefly discussed in Appendix C.

The discouraging feature of the Rice-Allnatt theory is that the predictions fall far short of the experimental values. One possible

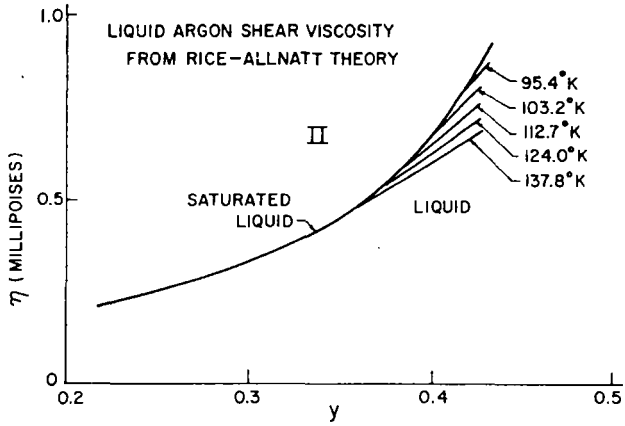

Figure 8. Isotherms for the liquid regime for the shear viscosity of argon, as predicted by the Rice–Allnatt theory (see Appendix B).

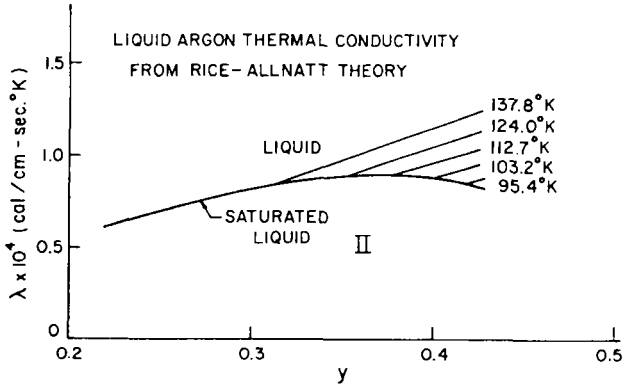

Figure 9. Isotherms for the liquid regime for the thermal conductivity c argon, as predicted by the Rice–Allnatt theory (see Appendix B).

reason for this is that pair correlation function data from the nonstable region of the YBG theory is used. Table 2 shows the effect of adjusting the parameters. With the new parameters, the Rice-Allnatt theory achieves approximately 65% of the experimental properties at 140.4 °K and 122.7 °K. Since the critical locus was used for scaling, and Fig. 3 shows coincidence of the adjusted and YBG curves at about 137 °K, it is not surprising that the results are somewhat better at 140.4 °K. The results of Table 1 further support the nature of these improvements.

TABLE 2 A table, corresponding to Table 1, showing the effect of adjusting the parameters on the prediction of the transport properties of saturated liquid argon.

		Before Adjustment			
ρ_m(g/cm³)	T (°K)	η_{RA}	η_{exp} (mp.)	λ_{RA}	λ_{exp} 10^{-4} (cal/cm. sec. °K)
1.16	120.3	0.465	1.08	0.898	2.0
1.42	86.2	0.895	2.75	0.821	3.05
		After Adjustment			
0.924	140.4	0.485	0.80	1.08	1.4
1.12	122.7	0.670	1.05	1.302	1.95

If one breaks down the transport coefficient into

$$\xi = \xi_{HS} + \xi_{attractive}$$

where $\xi = \eta, \lambda$, and ξ_{HS} is the Enskog dense gas of hard spheres contribution, one finds that

$$\xi_{SW} - \xi_{HS} > 0 \qquad \text{(square-well)}$$

in contrast to

$$\xi_{RA} - \xi_{HS} > 0 \qquad \text{(Rice-Allnatt)}$$

See Table 3.

This behavior is the visible reason why the predictions of the Rice-Allnatt theory are low. It is not clear to the authors whether a " well " should add or subtract from the hard sphere dense gas transport coefficients. The adjusting of the Rice-Allnatt theory does not alter this inequality. It appears that the two theories are not on an equal footing with respect to the hard sphere results. The para-

TABLE 3 A table showing the effects of subtracting the hard sphere contribution from the square-well and Rice–Allnatt transport coefficients. Units are mp. and 10^{-4} cal/cm. sec. °K respectively. $\theta = (T^*)^{-1}$ and $y = \pi n^*/6$.

SQUARE-WELL THEORY			
θ_{SW}	y_{SW}	$\eta_{SW} - \eta_{HS}$	$\lambda_{SW} - \lambda_{HS}$
0.5	0.26	0.38	0.30
	0.30	0.59	0.57
	0.34	0.85	0.90
	0.38	1.17	1.37
0.6	0.30	0.73	0.71
	0.34	1.05	1.12
	0.38	1.45	1.66
0.7	0.34	1.28	1.36
	0.38	1.75	1.98
RICE–ALLNATT THEORY			
θ_{RA}	y_{RA}	$\eta_{RA} - \eta_{HS}$	$\lambda_{RA} - \lambda_{HS}$
0.9	0.353	−0.521	−1.035
	0.428	−1.025	−2.108
1.0	0.428	−0.883	−2.050
1.1	0.428	−0.771	−2.009
1.2	0.428	−0.667	−1.968
1.3	0.428	−0.550	−1.919

meters σ in Rice-Allnatt and σ_1 in square-well have different meanings, since they are parameters in different intermolecular potential models.

4. Conclusion

Although the Rice-Allnatt theory has appealing trends with respect to the description of shear viscosity and thermal conductivity for liquids, it is not quantitatively as successful as the square-well theory, which exhibits incorrect trends in thermal conductivity at lower liquid temperatures. Furthermore, the square-well theory is easier to use. It is felt that one major difficulty with the Rice-Allnatt theory is the pair-correlation function data input. The method of adjusting the parameters is one suggestion for improving the data input.

Acknowledgement

The authors are grateful for support provided by the National Science Foundation (NSF Grant No. GK–14212) and the NSF Graduate Traineeship Program.

Appendix A: The Square-Well Transport Results[12,13]

Shear Viscosity:

$$\eta = \eta^* \left\{ \frac{[1 + \frac{8}{5} y (g(1) + R^3 g(R) \Psi)]^2}{g(1) + R^2 g(R) [\Xi + \frac{1}{6}\theta^2]} + \frac{768 y^2}{25\pi} (g(1) + R^4 g(R) \Xi) \right\} \tag{A–1}$$

Thermal Conductivity

$$\lambda = \lambda^* \left\{ \frac{[1 + \frac{12}{5} y (g(1) + R^3 g(R) \Psi)]^2}{g(1) + R^2 g(R) [\Xi + \frac{11}{16}\theta^2]} + \frac{512 y^2}{25\pi} (g(1) + R^4 g(R) \Xi) \right\} \tag{A–2}$$

where

$$\eta^* = \frac{5}{16\sigma_1^2} \left(\frac{mkT}{\pi} \right)^{1/2} \tag{A–3}$$

$$\lambda^* = \frac{75}{64\sigma_1^2} \left(\frac{k^3 T}{\pi m} \right)^{1/2} \tag{A–4}$$

$$\theta = \epsilon/kT = T^{*-1} \tag{A–5}$$

$$y = \pi n^*/6 \tag{A–6}$$

$$g(1) = g_{\mathrm{HS}}^{(2)}(x = 1)\, e^{\theta} \tag{A–7}$$

$$g(R) = g_{\mathrm{HS}}^{(2)}(x = R) \tag{A–8}$$

$$R = \sigma_2/\sigma_1 \tag{A–9}$$

$$\Psi = 1 - e^{\theta} + \frac{\theta}{2} \left[1 + \frac{4}{\sqrt{\pi}} e^{\theta} \int_{\sqrt{\theta}}^{\infty} e^{-x^2} x^2 \, dx \right] \tag{A–10}$$

$$\Xi = e^{\theta} - \frac{\theta}{2} - 2 \int_0^{\infty} x^2 (x^2 + \theta)^{1/2} e^{-x^2} \, dx \tag{A–11}$$

Appendix B: The Rice-Allnatt Transport Results[4,5,6,9]

Shear Viscosity:

$$\eta = \eta_K + \eta_V(R = \sigma) + \eta_V(R > \sigma) \tag{B-1}$$

$$\eta_K = \eta^* \left\{ \frac{1 + \frac{6}{5} y g^{(2)}(1)}{g^{(2)}(1) + 5\zeta_S^*/4} \right\} \tag{B-2}$$

$$\eta_V(R = \sigma) = \eta^* [4 y g^{(2)}(1)] \left\{ \tfrac{2}{5} \left(\frac{\eta_K}{\eta^*} \right) - \left(\frac{576}{25\pi} \right) y^2 \zeta_T^* \Psi^{(2)}(1) + \left(\frac{192}{25\pi} \right) y \right\} \tag{B-3}$$

$$\eta_V(R > \sigma) = \eta^* \left(\frac{9216}{25\pi} \right) \theta y^3 \zeta_T^* \int_1^\infty x^3 \phi'(x)\, \Psi^{(2)}(x) g^{(2)}(x)\, dx \tag{B-4}$$

Thermal Conductivity:

$$\lambda = \lambda_K + \lambda_V(R = \sigma) + \lambda_V(R > \sigma) \tag{B-5}$$

$$\lambda_K = \lambda^* \left\{ \frac{1 + \frac{12}{5} y g^{(2)}(1)}{g^{(2)}(1) + 45\zeta_S/16} \right\} \tag{B-6}$$

$$\lambda_V(R = \sigma) = \lambda^* [4 y g^{(2)}(1)] \left\{ \frac{128}{25\pi} y + \tfrac{3}{10} \left(\frac{\lambda_K}{\lambda^*} \right) \right\} \tag{B-7}$$

$$\lambda_V(R > \sigma) = \lambda^* (-256\theta y/25\zeta_T^*) \int_1^\infty x^2 g^{(2)}(x) \left[\phi(x) - \frac{x}{3} \phi'(x) - \frac{x}{3} (\phi(x) - x\phi'(x)) \frac{\partial}{\partial x} \right] \cdot \frac{\partial}{\partial \theta} (1 n g^{(2)}(x))\, dx \tag{B-8}$$

where θ, y, n^*, λ^* are defined in Appendix A, and

$$\phi(x) = x^{-12} - x^{-6} \tag{B-9}$$

$$\phi'(x) = d\phi(x)/dx \tag{B-10}$$

$g^{(2)}(x)$ = YBG pair correlation function for the modified Lennard-Jones 12–6 potential

ζ_S^* = reduced soft friction constant

$$= (\zeta_S/2mn\sigma^2) \left(\frac{m}{\pi k T} \right)^{1/2} \tag{B-11}$$

in which ζ_S is the soft friction constant computed by Helfand's linear trajectory approximation[15,16]

$$\zeta_T^* = \zeta_S^* + \zeta_H^* = \text{reduced total friction constant}$$

in which

$$\zeta_H^* = \text{reduced hard friction coefficient}$$

$$= \tfrac{4}{3} g^{(2)}(1) \tag{B-12}$$

The function $\Psi^{(2)}(x)$ is determined from the equation

$$\frac{\partial}{\partial x}\left[x^2 g^{(2)}(x) \frac{\partial \Psi^{(2)}}{\partial x}\right] - 6g^{(2)}(x)\, \Psi^{(2)}(x) - x^3 \frac{\partial g^{(2)}(x)}{\partial x} = 0 \tag{B-13}$$

$$\Psi^{(2)} = 0, x \to \infty \tag{B-14}$$

$$\frac{\partial \Psi^{(2)}}{\partial x} = 0, x \to 1_+ \tag{B-15}$$

The above presentation of the Rice-Allnatt theory incorporates the modification to the theory by Wei and Davis[9,17,18]; specifically, the modification entails the use of ζ_T^* instead of ζ_S^* in the λ_V and η_V contributions.

Appendix C: Comments on the Rice-Allnatt Computations

As mentioned in Appendix B, the Wei–Davis[9,17,18] modifications were incorporated into the Rice-Allnatt theory used in this paper. Allowing this, all thermal conductivity computations are consistent with previously existing computations.

Disagreement was found with the $\Psi^{(2)}(x)$ function computation presented in Eq. (B–13) to (B–15) and which result appears in Eq. (B–3) and (B–4). The computational scheme followed is presented in Rice and Gray.[4] An example of the conflict of results is

At	$\theta = 0.968$ and	$y = 0.353$
Rice *et al.*[4]	$\Psi^{(2)}(1) = -0.106$;	$P = 4.39$
This paper	$= +0.0462$;	$= 0.198$

Recognizing this computation as a sensitive one, the authors refined the pair correlation function data of Kirkwood *et al.*[2] This refinement did not alter the result significantly.

The effect of the above discrepancy in $\Psi^{(2)}(x)$ is to cause a decrease in the predicted value of shear viscosity.

REFERENCES

1. Callen, H. B., *Thermodynamics*, pp. 146–154, John Wiley & Sons, Inc., 1960.
2. Kirkwood, J. G., Lewison, V. A. and Alder, B. J., *J. Chem. Phys.* **20**, 929 (1962).
3. Hill, T. L., *Statistical Mechanics*, pp. 204–209, McGraw-Hill Book Co., Inc., 1956.
4. Rice, S. A. and Gray, P., *The Statistical Mechanics of Simple Liquids*, Chapters 5 and 6, Interscience Publications, Inc., 1965.
5. Rice, S. A. and Allnatt, A. R., *J. Chem. Phys.* **34**, 2144 (1961).
6. Allnatt, A. R. and Rice, S. A., *J. Chem. Phys.* **34**, 2156 (1961).
7. Rovner, J. M., M.S. Thesis (U. of Minnesota, 1969).
8. Tan, P. Y. and Luks, K. D. (unpublished).
9. For example, see " Comments on the Experimental and Theoretical Study of Transport Phenomena in Simple Liquids " by Rice, S. A., Boon, J. P. and Davis, H. T., in *Simple Dense Fluids*, ed. by Frisch, H. L. and Salsburg, Z. W., Academic Press, 1968.
10. Diller, D. E., Hanley, H. J. M. and Roder, H. M., *Cryogenics*, p. 286, August, 1970.
11. Davis, H. T., Rice, S. A. and Sengers, J. V., *J. Chem. Phys.* **35**, 2210 (1961),
12. Davis, H. T. and Luks, K. D., *J. Phys. Chem.* **69**, 869 (1965).
13. Luks, K. D., Miller, M. A. and Davis, H. T., *J. A.I.Ch.E.* **12**, 1079 (1966).
14. Hirschfelder, J. O., Curtiss, C. F. and Bird, R. B., *Molecular Theory of Gases and Liquids*, pps. 634–652, John Wiley & Sons, Inc. 1964.
15. Helfand, E., *Phys. of Fluids* **4**, 681 (1961).
16. Palyvos, J. A. and Davis, H. T., *J. Phys. Chem.* **71**, 439 (1967).
17. Wei, C. A. and Davis, H. T., *J. Chem. Phys.* **45**, 2533 (1966).
18. Wei, C. C. and Davis, H. T., *J. Chem. Phys.* **46**, 3456 (1967).
19. Ikenberry, L. D. and Rice, S. A., *J. Chem. Phys.* **39**, 1561 (1963).
20. Cook, G. A., *Argon, Helium and the Rare Gases*, Vol. I, John Wiley & Sons, Inc., 1961.
21. de Bock, A., Grevendonk, W. and Herreman, W., *Physica* **37**, 227 (1967).